

Model independent study of the nucleon self-energy in matter

O. Pohl, C. Fuchs and A. Faessler

Institut für Theoretische Physik, Universität Tübingen, Auf der Morgenstelle 14, D-72076
Tübingen, Germany

ABSTRACT

Relativistic and non-relativistic modern nucleon-nucleon potentials are mapped on a relativistic operator basis using projection techniques. This allows to compare the various potentials at the level of covariant amplitudes where a remarkable agreement is found. In nuclear matter large scalar and vector mean fields of several hundred MeV magnitude are generated at tree level. This is found to be a model independent feature of the nucleon-nucleon interaction.

I. INTRODUCTION

A fundamental question in nuclear physics is the role which relativity plays in nuclear systems. The ratio of the Fermi momentum over the nucleon mass is about $k_F/M \simeq 0.25$ and nucleons move thus with maximally about 1/4 of the velocity of light which implies only moderate corrections from relativistic kinematics. However, there exists a fundamental difference between relativistic and non-relativistic dynamics: a genuine feature of relativistic nuclear dynamics is the appearance of large scalar and vector mean fields, each of the magnitude of several hundred MeV. The scalar field Σ_S is attractive and the vector field Σ_μ is repulsive. In relativistic mean field (RMF) theory, both, sign and size of the fields are enforced by the nuclear saturation mechanism [1].

At nuclear saturation density $\rho_0 \simeq 0.16 \text{ fm}^{-3}$ the empirical fields deduced from RMF fits to finite nuclei are of the order of $\Sigma_s \simeq -350 \text{ MeV}$ and $\Sigma_o \simeq +300 \text{ MeV}$ [2] (Σ_o is the time-like component of Σ_μ). The single particle potential in which the nucleons move originates from the cancellation of the two contributions $U_{\text{s.p.}} \simeq \Sigma_o + \Sigma_s \simeq -50 \text{ MeV}$ which makes it difficult to observe relativistic effects in nuclear systems. There exist, however, several features in nuclear structure which can naturally be explained within Dirac phenomenology while models based on non-relativistic dynamics have difficulties. Best established is the large *spin-orbit splitting* in finite nuclei. Also the so-called *pseudo-spin symmetry*, observed more than thirty years ago in single-particle levels of spherical nuclei, can naturally be understood within RMF theory as a consequence of the coupling to the lower components of the Dirac equation [3].

A connection to Quantum-Chromo-Dynamics (QCD) as the fundamental theory of strong interactions is established by QCD sum rules [4, 5]. The change of the chiral condensates $\langle \bar{q}q \rangle, \langle q^\dagger q \rangle$ in matter leads to attractive scalar and repulsive vector self-energies which are astonishingly close to the empirical values derived from RMF fits to the nuclear chart. Also relativistic many-body calculations [6, 7, 8] yield scalar/vector fields of the same sign and magnitude as obtained from RMF theory or, alternatively, from QCD sum rules. Moreover, Dirac-Brueckner-Hartree-Fock (DBHF) calculations [7] agree even quantitatively surprisingly well with the QCD motivated approach of Ref. [9] where chiral fluctuations from pion-nucleon dynamics were considered on top of the chiral condensates.

These facts suggest that preconditions for the existence of large fields in matter or, alternatively, the density dependence of the QCD condensates, must already be inherent in the vacuum nucleon-nucleon (NN) interaction.

Relativistic one-boson-exchange potentials (OBEP), e.g. Bonn (A,B,C), [10] provide fits with fair precision to NN scattering data as well as the non-relativistic meson-theoretical Nijmegen soft-core potential Nijm93 [13]. High precision fits (with $\chi^2/\text{datum} \simeq 1.01$) are

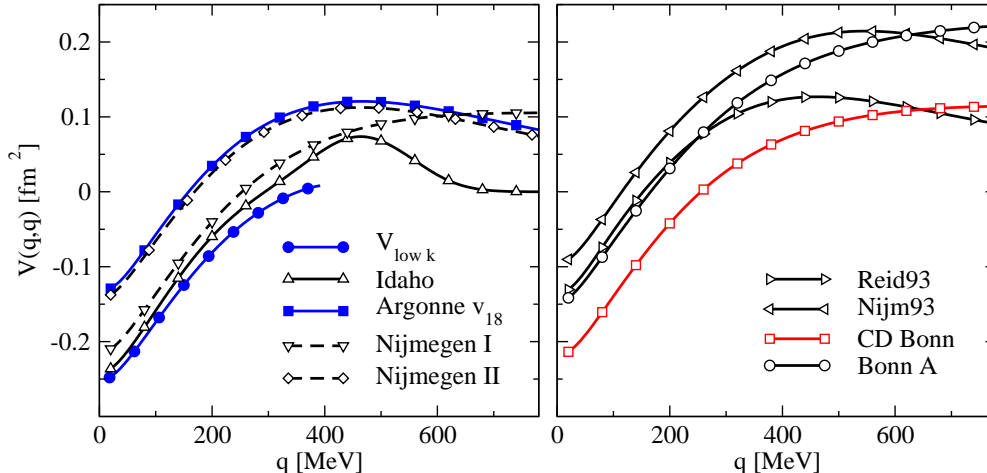


FIG. 1: Diagonal matrix elements $V(\mathbf{q}, \mathbf{q})$ in the 1S_0 partial wave $V(\mathbf{q}, \mathbf{q})$ for different high precision NN potential models.

provided by OBE type potentials such as the relativistic CD-Bonn [11] or the non-relativistic Nijmegen potentials Nijm I and Nijm II [13] where fits are performed separately in each partial wave. In contrast to e.g. the spectator model of [14] the 'standard' OBE potentials are based on the no-sea approximation which excludes explicit excitations of anti-nucleons but absorbs such contributions into the model parameters, in particular into a large ω coupling. The present investigations are restricted to the standard-type models.

The long-range part of the interaction is generally mediated by the one-pion-exchange (OPE) while the scalar intermediate range attraction is mainly due to correlated two-pion-exchange. The short-range part, i.e. the hard core, is dominated by vector meson exchange, i.e. the isoscalar ω and the isovector ρ meson. Widely used in nuclear physics are, however, also high precision non-relativistic empirical potentials such as the Argonne potential AV_{18} [15] or the Reid93 potential [13]. A systematic connection to QCD is established by chiral effective field theory (EFT). Up to now the two-nucleon system has been considered at next-to-next-to-next-to-leading order (N^3LO) in chiral perturbation theory [16, 17]. In such approaches the NN potential consists of one-, two- and three-pion exchanges and regularizing contact interactions which account for the short-range correlations. The advantage of EFT compared to the more phenomenological OBE potentials is the systematic expansion in terms of chiral power counting.

A better understanding of the common features of the various approaches is essential in order to arrive at a more model independent understanding of the nucleon-nucleon interaction, in particular since all well established interactions fit NN scattering data with approximately the same precision. Substantial progress was recently achieved by the construction of a universal low energy NN potential $V_{low\ k}$ based on renormalization group

techniques [18]. However, like the EFT potentials $V_{\text{low } k}$ is not covariantly formulated and has therefore not been used in relativistic nuclear structure calculations.

The present work applies projection techniques to map the various potentials on the operator basis of relativistic field theory which is given by the Clifford algebra in Dirac space. This allows to identify the different Lorentz components of the interaction and to calculate the relativistic self-energy operator in matter. The basic results of our approach have been presented in [19]. A more extended investigation is in preparation. The philosophy behind this approach is based on the fact, that any NN interaction, whether relativistic or not, is based on a common spin-isospin operator structure which invokes certain scales: long-range spin-isospin dependent forces, essentially given by the one-pion exchange, short- and intermediate-range spin-independent interactions, short-range isoscalar spin-orbit interactions and quadratic isovector spin-orbit interactions.

II. COVARIANT AMPLITUDES

In a covariant formulation the spin-isospin structure of the interaction is constrained by the symmetries of the Lorentz group. E.g. the Born scattering matrix of covariant OBE potentials is given by the sum over the corresponding scalar, pseudoscalar and vector mesons α

$$\hat{V}(q', q) = \sum_{\alpha=s,ps,v} \mathcal{F}_\alpha^2(q', q) \Gamma_\alpha^{(2)} D_\alpha(q' - q) \Gamma_\alpha^{(1)} , \quad (1)$$

where q_μ and q'_μ are the c.m. momenta of the incoming and outgoing nucleons. \mathcal{F}_α are form factors applied to the vertices Γ_α . The meson propagators read

$$D_{s,ps}(q' - q) = i \frac{1}{(q' - q)^2 - m_{s,ps}^2} \quad (2)$$

$$D_v^{\mu\nu}(q' - q) = i \frac{-g^{\mu\nu} + (q' - q)^\mu (q' - q)^\nu / m_v^2}{(q' - q)^2 - m_v^2} \quad (3)$$

for scalar and pseudoscalar mesons s, ps and vector mesons v . Isospin factors ($\boldsymbol{\tau}_1 \cdot \boldsymbol{\tau}_2$) are suppressed in (1). The Dirac structure of the potential is contained in the meson-nucleon vertices

$$\Gamma_s = g_s \mathbf{1}, \quad \Gamma_{ps} = g_{ps} \frac{\not{q}' - \not{q}}{2M} i\gamma_5, \quad \Gamma_v = g_v \gamma^\mu + \frac{f_v i\sigma^{\mu\nu}}{2M} . \quad (4)$$

For the pseudoscalar mesons π and η a pseudovector coupling is used and the ω meson has no tensor coupling, i.e. $f_v^{(\omega)} = 0$. The potential $V(\mathbf{q}', \mathbf{q})$, i.e. the OBE Feynman amplitudes are obtained by sandwiching \hat{V} between the incoming and outgoing Dirac spinors.

From a low energy expansion of the full field-theoretical OBE Feynman amplitudes into a set of spin and isospin operators one obtains the representation of non-covariant potentials

$$V = \sum_i [V_i + V'_i \boldsymbol{\tau}_1 \cdot \boldsymbol{\tau}_2] O_i. \quad (5)$$

where the operators O_i , assuming identical particle scattering and charge independence, are given by

$$\begin{aligned} O_1 &= 1, \\ O_2 &= \boldsymbol{\sigma}_1 \cdot \boldsymbol{\sigma}_2, \\ O_3 &= (\boldsymbol{\sigma}_1 \cdot \mathbf{k})(\boldsymbol{\sigma}_2 \cdot \mathbf{k}), \\ O_4 &= \frac{i}{2}(\boldsymbol{\sigma}_1 + \boldsymbol{\sigma}_2) \cdot \mathbf{n}, \\ O_5 &= (\boldsymbol{\sigma}_1 \cdot \mathbf{n})(\boldsymbol{\sigma}_2 \cdot \mathbf{n}), \end{aligned} \quad (6)$$

where $\mathbf{k} = \mathbf{q}' - \mathbf{q}$, $\mathbf{n} = \mathbf{q} \times \mathbf{q}' \equiv \mathbf{P} \times \mathbf{k}$ and $\mathbf{P} = \frac{1}{2}(\mathbf{q} + \mathbf{q}')$ is the average momentum. The potential forms V_i are then functions of \mathbf{k} , \mathbf{P} , \mathbf{n} and the energy. In order to perform a non-relativistic reduction, usually the energy E is expanded in \mathbf{k}^2 and \mathbf{P}^2

$$E(\mathbf{q}) = \left(\frac{\mathbf{k}^2}{4} + \mathbf{P}^2 + M^2 \right)^{\frac{1}{2}} \simeq m + \frac{\mathbf{k}^2}{8M} + \frac{\mathbf{P}^2}{2M}. \quad (7)$$

and terms to leading order in \mathbf{k}^2/M^2 and \mathbf{P}^2/M^2 are taken into account. The meson propagators $D_\alpha(q' - q)$ given in Equation (2) and (3) are approximated by their static form.

The modern non-covariant Nijm 93 as well as the Nijm I and II potentials are constructed from approximate OBE amplitudes and thus based on the operator structure (6). However, since they are separately fitted in each partial wave (except Nijm 93) they are often referred to as phenomenological models. The Argonne AV₁₈ [15] and the Reid93 potential are purely phenomenological in the sense that the OBE picture is released. Based on the symmetries of (6), the intermediate and short-range part is parameterised by phenomenological functions V_α and only one-pion-exchange is contained explicitly. The EFT potentials, containing one- and multi-pion exchange explicitly, are even more rigorous since most part of the nuclear repulsion is carried by regularizing counter terms. Such an approach is justified by the fact that heavy meson (ρ, ω) exchange cannot be resolved up to the momentum scale of about 400 MeV which is constrained by NN scattering data. We apply the EFT Idaho potential [16] which fits NN scattering data with similar quality as AV₁₈ or the Nijmegen potentials. The same philosophy is behind $V_{\text{low } k}$ which can be viewed as the condensation of the various formulations to a model independent result.

Although based on the same operator structure as OBEPs, it is not straightforward to fix the Lorentz character of the various pieces of the non-covariant interactions AV₁₈, Reid93, EFT (Idaho) and $V_{\text{low } k}$.

However, any two-body amplitude can be represented covariantly by Dirac operators and Lorentz invariant amplitudes [20]. A relativistic treatment invokes automatically the excitation of anti-nucleons. However, NN scattering, in both, relativistic and non-relativistic approaches is restricted to the positive energy sector and neglects the coupling to anti-nucleons. As a consequence one has to work in a subspace of the full Dirac space where on-shell two-body matrix elements can be expanded into five Lorentz invariants. A possible choice of a set of five linearly independent covariant operators are the scalar, vector, tensor, axial-vector and pseudo-scalar Fermi covariants

$$\Gamma_m = \{S, V, T, P, A\} \quad (8)$$

with

$$S = \mathbf{1} \otimes \mathbf{1}, \quad V = \gamma^\mu \otimes \gamma_\mu, \quad T = \sigma^{\mu\nu} \otimes \sigma_{\mu\nu}, \quad P = \gamma_5 \otimes \gamma_5, \quad A = \gamma_5 \gamma^\mu \otimes \gamma_5 \gamma_\mu. \quad (9)$$

Working with physical, i.e. antisymmetrized matrix elements V^A , one has to keep in mind that direct and exchange covariants $\tilde{\Gamma}_m$ (where Dirac indices of particles 1 and 2 are interchanged) are coupled by a Fierz transformation. Since the low momentum part of the NN interaction is totally dominated by the pseudovector one-pion exchange (OPE) it is preferable to choose an operator basis where the pseudovector exchange is completely separated from the remaining operator structure and allows thus a more transparent investigation of the short- and intermediate-range parts of the potentials which are actually the interesting ones.

This can be achieved by the following set of covariants originally proposed by Tjon and Wallace [20]

$$\Gamma_m = \{S, -\tilde{S}, (A - \tilde{A}), PV, -\tilde{P}\tilde{V}\}. \quad (10)$$

PV and $\tilde{P}\tilde{V}$ are the direct and exchange pseudovector covariants, analogous to the pseudoscalar covariant P, however, with γ_5 replaced by $(\not{q}' - \not{q})/2M\gamma_5$. Thus the on-shell ($|\mathbf{q}| = |\mathbf{q}'|$) scattering matrix is given by

$$\hat{V}^I(\mathbf{q}', \mathbf{q}) = \sum_m g_m^I(|\mathbf{q}|, \theta) \Gamma_m, \quad (11)$$

where θ is the c.m. scattering angle and $I = 0, 1$ the isospin channel. For the Hartree-Fock self-energy it is sufficient to consider $\theta = 0$ when antisymmetrized matrix elements are used since $\theta = \pi$ contains then only redundant information. The transformation of the Born amplitudes from an angular-momentum basis of a given NN potential, where the 1S_0 partial wave of the studied potentials is shown in Fig. 1, onto the covariant basis (11) is now standard and runs over the following steps:

$|LSJ\rangle \rightarrow$ partial wave helicity states \rightarrow plane wave helicity states \rightarrow covariant basis.

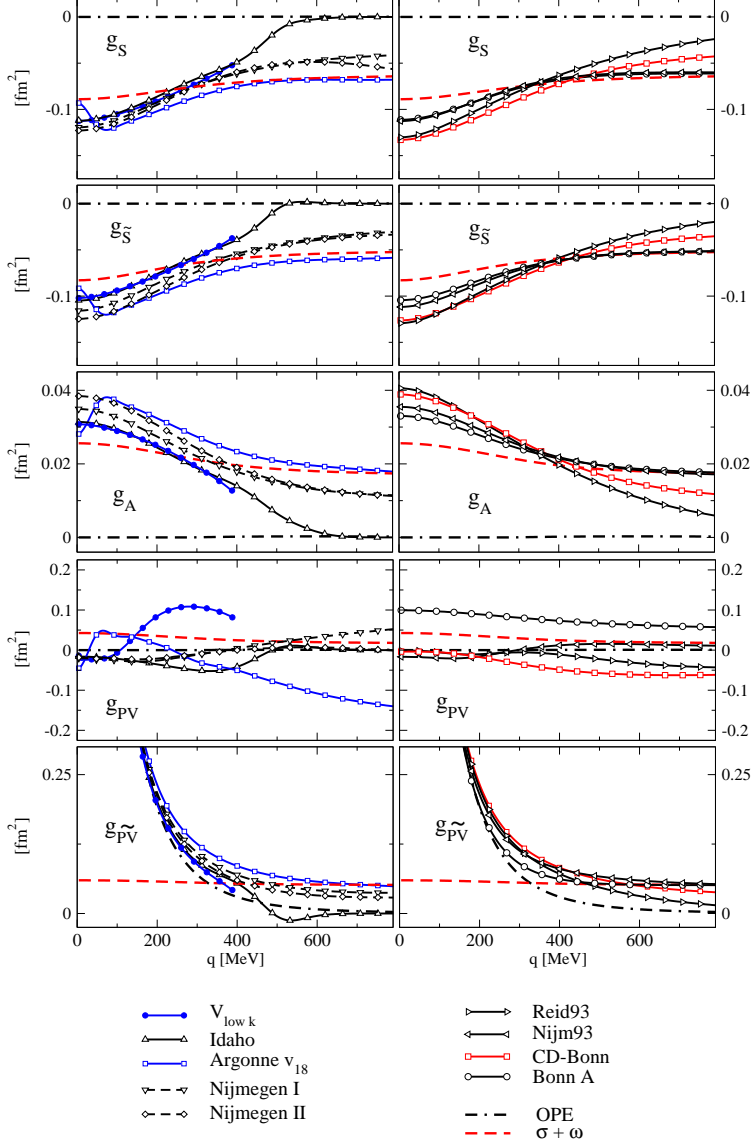


FIG. 2: Isospin-averaged Lorentz invariant amplitudes $g_m^D(|\mathbf{p}|, \theta = 0)$ for the different NN potentials after projection on the Dirac operator structure. The pseudovector representation of the relativistic operator basis is used. As a reference the amplitudes from solely OPE and from $\sigma + \omega$ exchange, both with Bonn A parameters, are shown.

The first two transformation can e.g. be found in Refs. [21]. The last step has to be performed numerically by matrix inversion [7, 22].

Fig. 2 shows the resulting isospin-averaged amplitudes $g_m = \frac{1}{2}(g_m^{I=0} + 3g_m^{I=1})$ at $\theta = 0$ for the various potentials. Since these amplitudes are not very transparent quantities, Fig. 2 includes as a reference in addition the contributions from only OPE and from only σ and ω exchange, both taken from Bonn A. The four amplitudes g_S , $g_{\tilde{S}}$, g_A and $g_{\tilde{P}V}$ are very close

for the OBEPs Bonn A, Nijm 93, CD-Bonn, Nijmegen I and II, and the non-relativistic AV_{18} , Reid93, Idaho and $V_{\text{low } k}$. The direct pseudovector amplitude g_{PV} falls somewhat out of systematics. This amplitude is, however, of minor importance since it does not contribute to the Hartree-Fock self-energy (12) and to the single particle potential. The dominance of the OPE at low $|\mathbf{q}|$ is reflected in the pseudovector exchange amplitude $g_{\widetilde{\text{PV}}}$ which is at small $|\mathbf{q}|$ almost two orders of magnitude larger than the other amplitudes.

For the covariant OBEPs Bonn and CD-Bonn and the OBE-like Nijmegen potentials a coincidence at the level of covariant amplitudes is not completely unexpected. However, it is remarkable that this agreement transfers to the EFT Idaho potential and also to $V_{\text{low } k}$ which are of completely different character and theoretical background.

The high momentum part of the interaction, on the other hand, is dominated by heavy meson exchange in the OBEPs and the corresponding amplitudes g_S , $g_{\overline{S}}$, g_A approach the $\sigma + \omega$ exchange result. This is also true for AV_{18} and Reid93 which could not have been expected a priori. Deviations from the $\sigma + \omega$ amplitudes, e.g. due to exchange of isovector mesons ρ and δ in the OBEPs or the corresponding isovector operators in AV_{18} are moderate at large $|\mathbf{q}|$. These deviations are more pronounced at small $|\mathbf{q}|$. In summary we find a remarkable agreement between the OBE amplitudes and those derived from AV_{18} or Reid93. This means that for on-shell scattering AV_{18} can be mapped on the relativistic operator structure where the local phenomenological functions V_i , Eq. (5), play the same role as the meson propagators plus corresponding form factors in the meson exchange picture.

Turning now to the chiral Idaho potential, where the momentum-space NN amplitude is also based on the operator structure given in Eq. 6, the situation is different. At low $|\mathbf{q}|$ the amplitudes derived from the Idaho potential behave qualitatively and quantitatively like the previous ones, i.e., they are very close to Bonn A, CD-Bonn and AV_{18} . Again we would conclude that also the chiral potential can be mapped on a relativistic operator structure. The functions V_i and V'_i in combination with the corresponding operators, derived from fourth order 2π exchange plus contact terms, lead to a structure which is similar to that one imposed by the OBE picture. However, clear deviations appear in the cut-off region between 400 and 500 MeV. The short-range interactions are strongly suppressed by the exponential cut-off form factors and as a consequence the Idaho approaches rapidly the OPE result for momenta above 400 MeV. The $V_{\text{low } k}$ potential is only displayed up to a momentum of 400 MeV since the high momentum nodes are integrated out down to a scale of $\Lambda = 2.1 fm^{-1}$ in order to arrive at a low-momentum potential. It shows a similar behaviour compared to the other potential models especially when compared to the chiral EFT potential. As in the chiral EFT potential where the short-range physics is absorbed in contact terms, the unresolved short-range part is removed and replaced by contact interactions. Therefore when going to higher $|\mathbf{q}|$ the amplitudes of the $V_{\text{low } k}$ potential deviate from the $\sigma + \omega$

exchange. Nevertheless the $V_{\text{low } k}$ matrix elements are provided in numerical rather than analytical form. When mapped on a general relativistic operator basis one finds that the Dirac structure is comparable to that of the chiral EFT potential, the relativistic and non-relativistic OBEPs and phenomenological potentials.

III. SELF-ENERGY

With the covariant amplitudes at hand, one is now able to determine the relativistic mean field in nuclear matter by calculating the relativistic self-energy Σ in Hartree-Fock approximation at *tree level*. We are thereby not aiming for a realistic description of nuclear matter saturation properties which would require a self-consistent scheme. Moreover, short-range correlations require to base such calculations on the in-medium T-matrix rather than the bare potential V [23]. This leads to the relativistic Dirac-Brueckner-Hartree-Fock scheme which has been proven to describe nuclear saturation with quantitatively satisfying accuracy [6, 7, 8].

The self-energy for the nucleon k follows from the interaction matrix V by integrating over the occupied states q in the Fermi sea

$$\Sigma_{\alpha\beta}(k, k_F) = -i \int \frac{d^4q}{(2\pi)^4} G_{\tau\sigma}^D(q) V^A(k, q)_{\alpha\sigma;\beta\tau}. \quad (12)$$

The Dirac propagator

$$G^D(q) = [\not{q} + M] 2\pi i \delta(q^2 - M^2) \Theta(q_0) \Theta(k_F - |\mathbf{q}|) \quad (13)$$

describes the on-shell propagation of a nucleon with momentum \mathbf{q} and energy $E_{\mathbf{q}} = \sqrt{\mathbf{q}^2 + M^2}$ inside the Fermi sea. In isospin saturated nuclear matter the self-energy consists of a scalar Σ_s , a time-like vector Σ_o and a spatial vector part Σ_v

$$\Sigma(k, k_F) = \Sigma_s(k, k_F) - \gamma_0 \Sigma_o(k, k_F) + \boldsymbol{\gamma} \cdot \mathbf{k} \Sigma_v(k, k_F), \quad (14)$$

which are given by [7]

$$\begin{aligned} \Sigma_s &= \frac{1}{4} \int^{k_F} \frac{d^3\mathbf{q}}{(2\pi)^3} \frac{M}{E_{\mathbf{q}}} \left[4g_S - g_{\tilde{S}} + 4g_A - \frac{(k^\mu - q^\mu)^2}{4M^2} g_{\tilde{P}\tilde{V}} \right], \\ \Sigma_o &= \frac{1}{4} \int^{k_F} \frac{d^3\mathbf{q}}{(2\pi)^3} \left[g_{\tilde{S}} - 2g_A + \frac{E_{\mathbf{k}} (k^\mu - q^\mu)^2}{E_{\mathbf{q}} 4M^2} g_{\tilde{P}\tilde{V}} \right] \\ \Sigma_v &= \frac{1}{4} \int^{k_F} \frac{d^3\mathbf{q}}{(2\pi)^3} \frac{\mathbf{k} \cdot \mathbf{q}}{|\mathbf{k}|^2 E_{\mathbf{q}}} \left[g_{\tilde{S}} - 2g_A + \frac{k_z (k^\mu - q^\mu)^2}{q_z 4M^2} g_{\tilde{P}\tilde{V}} \right]. \end{aligned} \quad (15)$$

Fig. 3 (a) shows the tree level self-energy components obtained with the various potentials in nuclear matter at saturation density with a Fermi momentum $k_F = 1.35 \text{ fm}^{-1}$. All

potentials yield scalar and vector fields Σ_s and Σ_o of comparable strength: a large and attractive scalar field $\Sigma_s \simeq -(450 \div 400)$ MeV and a repulsive vector field of $\Sigma_o \simeq +(350 \div 400)$ MeV. These values are comparable to those derived from RMF phenomenologically

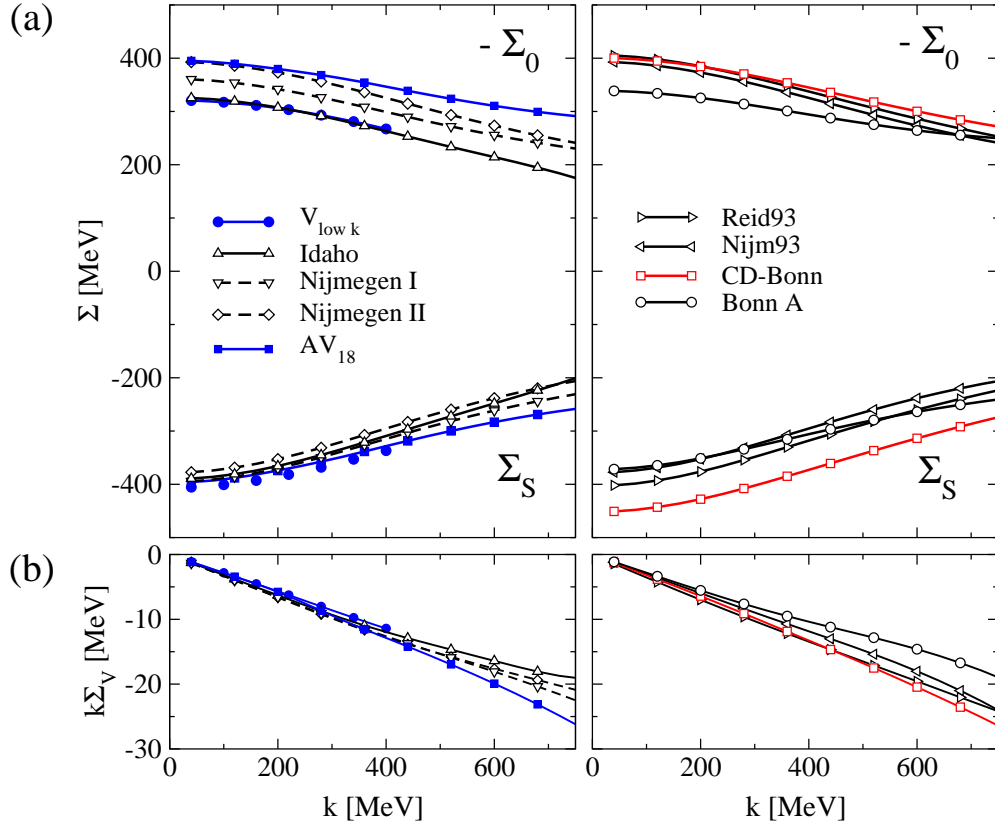


FIG. 3: Tree level results for (a) the scalar Σ_v and vector Σ_o self-energy components and (b) spatial vector self-energy component $k\Sigma_v$ in nuclear matter at $k_F = 1.35 \text{ fm}^{-1}$ for the different NN interaction models.

and also from QCD sum rules. Also the explicit momentum dependence of the self-energy is similar for the various potentials. The Idaho mean fields follow the other approaches at low k but show a stronger decrease above $k \simeq 2 \text{ fm}^{-1}$ which reflects again the influence of the cut-off parameter. The spatial components $k\Sigma_v$ are shown in Fig. 3 (b). Also here the various potentials agree quite well.

As known from self-consistent DBHF calculations [6, 7], the spatial vector self-energy is a moderate correction to the large scalar and time-like vector components Σ_s and Σ_o . This is already the case at tree level where $k\Sigma_v$ is about one order of magnitude smaller than the other two components. The spatial self-energy originates exclusively from exchange contributions, i.e., the Fock term, and vanishes ,e.g., in the mean field approximation of RMF theory.

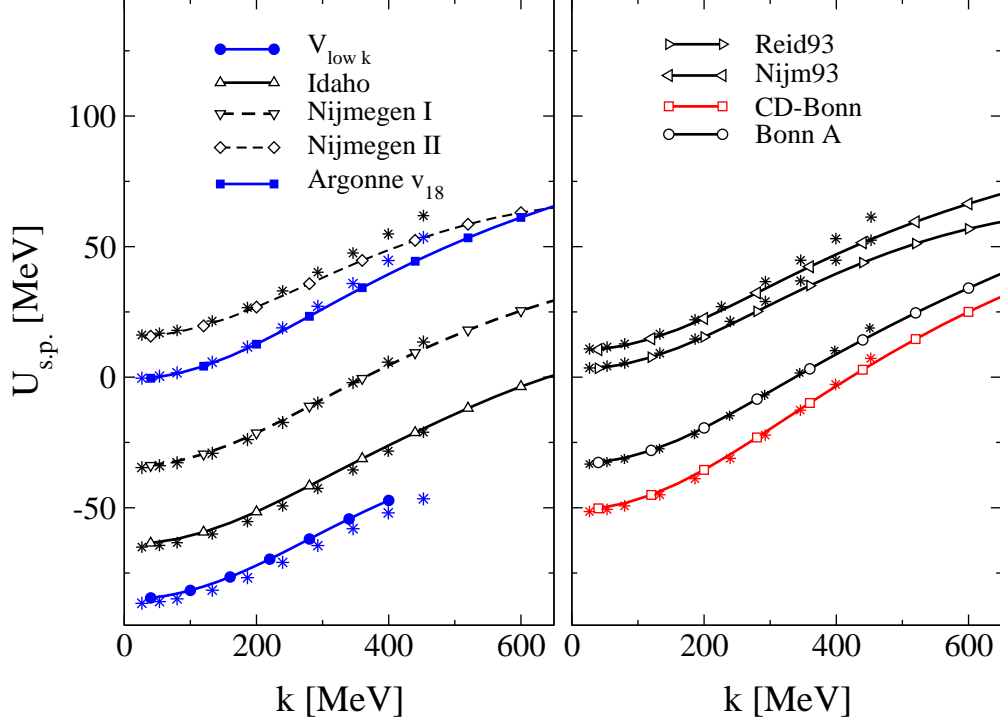


FIG. 4: Single particle potential in nuclear matter at $k_F = 1.35 \text{ fm}^{-1}$, determined from the tree level Born amplitudes of the various potentials. The single particle potential determined from the relativistic self-energy components after projection onto the covariant operator basis is compared to a non-relativistic calculation (stars) where partial wave amplitudes are summed up directly.

In Fig. 4 the single particle potential is shown, which is defined as the expectation value of the self-energy Σ

$$U_{\text{s.p.}}(k) = \frac{\langle u(k) | \gamma^0 \Sigma | u(k) \rangle}{\langle u(k) | u(k) \rangle} = \frac{M}{E(\mathbf{k})} \langle \bar{u}(k) | \Sigma | u(k) \rangle \quad (16)$$

and reads

$$U_{\text{s.p.}}(k, k_F) = \frac{M}{E} \Sigma_s - \frac{k_\mu \Sigma^\mu}{E} = \frac{M \Sigma_s}{\sqrt{\mathbf{k}^2 + M^2}} - \Sigma_o + \frac{\Sigma_v \mathbf{k}^2}{\sqrt{\mathbf{k}^2 + M^2}} \quad (17)$$

It reflects the well known fact that various two-body potentials are rather different although they are phase-shift equivalent, i.e. they describe NN scattering data with about the same accuracy when iterated in the Lippmann-Schwinger equation [23]. The differences at tree level are mainly due to differences in the short-range part of the interaction [18]. Fig. 4 includes also the results from a 'non-relativistic' calculation of $U_{\text{s.p.}}$ where the partial wave amplitudes are directly summed up. In particular at low momenta the non-relativistic and the relativistic calculations show an excellent agreement which demonstrates the accuracy of the applied projection techniques.

In order to estimate the influence of short-range correlations and self-consistency, Fig.

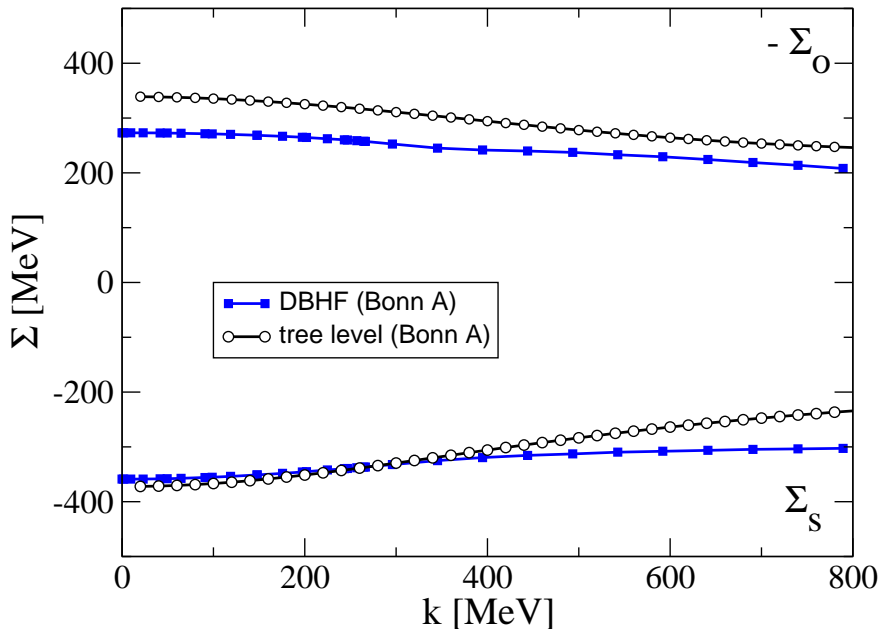


FIG. 5: Tree level scalar and vector self-energy components in nuclear matter at $k_F = 1.35 \text{ fm}^{-1}$ are compared to corresponding values from a full self-consistent relativistic Brueckner (DBHF) calculation. In both cases the Bonn A potential is used.

5 compares the tree level result from Fig. 3 for Bonn A to a corresponding full DBHF calculation at $k_F = 1.35 \text{ fm}^{-1}$. For DBHF the approach of [7] is used (subtracted T-matrix in pv representation). The DBHF calculation yields reasonable saturation properties with a binding energy of $E_{\text{bind}} = -15.72 \text{ MeV}$ and a saturation density of $\rho = 1.84 \text{ fm}^{-3}$ [7]. It is no doubt that higher order correlations are essential for saturation of nuclear matter. The correlations lead to a general reduction of the vector self-energy by a shift of about 50 MeV. Self-consistency and correlations also weakens the momentum dependence, in particular for Σ_s . However, except of the 50 MeV shift of Σ_o , the absolute magnitude of the self-energies is not strongly modified in the realistic calculation. This means that one can expect that the large attractive scalar and repulsive vector mean fields will also persist for the other interactions when short-range correlations are accounted for in a full relativistic many-body calculation.

IV. SUMMARY

We presented a model independent study of the Dirac structure of the nucleon-nucleon interaction. The potentials were projected on a relativistic operator basis in Dirac space using standard projection techniques which transform from a partial wave basis, where the potentials are originally given, to the basis of covariant amplitudes. The different approaches can now be compared at the level of these covariant amplitudes and, moreover, this allows to calculate the relativistic self-energy operator in nuclear matter. For both, the covariant amplitudes and the tree-level Hartree-Fock self-energy, we observe a remarkable agreement between the OBEPs (Bonn, CD-Bonn, Nijmegen), the phenomenological AV_{18} and Reid93 potentials and the EFT based Idaho and $V_{\text{low } k}$ potentials. The structure of the interaction enforces the existence of large scalar and vector fields as a model independent fact. The scale of these fields is set at the tree level. Although essential for nuclear binding and saturation, higher order correlations, i.e. Brueckner ladder correlations, change the size of the fields by less than 20% [7]. The magnitude of the fields is similar to that predicted by relativistic mean field phenomenology, relativistic many body correlations and also by QCD sum rules. We conclude that the appearance of large scalar and vector fields in matter is a general and model independent consequence of the vacuum structure of the NN interaction. Relativistic dynamics is therefore essential for nuclear systems.

-
- [1] B.D. Serot, J.D. Walecka, *Adv. Nucl. Phys.* **16**, 1 (1986).
 - [2] P. Ring, *Prog. Part. Nucl. Phys.* **73**, 193 (1996).
 - [3] J.N. Ginocchio, *Phys. Rev. Lett.* **78**, 436 (1997).
 - [4] T.D. Cohen, R.J. Furnstahl, D.K. Griegel, *Phys. Rev. Lett.* **67**, 961 (1991); *Phys. Rev. C* **45**, 1881 (1992).
 - [5] E.G. Drukarev, E.M. Levin, *Prog. Part. Nucl. Phys.* **27**, 77 (1991).
 - [6] B. ter Haar and R. Malfliet, *Phys. Rep.* **149**, 207 (1987).
 - [7] T. Gross-Boelting, C. Fuchs, and Amand Faessler, *Nucl. Phys.* **A648**, 105 (1999).
 - [8] E. van Dalen, C. Fuchs, A. Faessler, *Nucl. Phys.* **A744** 227 (2004); *Phys. Rev. Lett.* **95**, 022302 (2005).
 - [9] P. Finelli, N. Kaiser, D. Vretenar, W. Weise, *Nucl. Phys.* **A735**, 449 (2004).
 - [10] R. Machleidt, K. Holinde, Ch. Elster, *Phys. Rep.* **149**, 1 (1987).
 - [11] R. Machleidt, *Phys. Rev. C* **63**, 024001 (2001).

- [12] V.G.J. Stoks, R.A.M. Klomp, M.C.M. Rentmeester, J.J. de Swart Phys. Rev. C **48**, 792 (1993).
- [13] V.G.J. Stoks, R.A.M. Klomp, C.P.F. Terheggen, and J.J. de Swart Phys. Rev. C **49**, 2950 (1994).
- [14] F. Gross, J.W. Van Orden, K. Holinde Phys. Rev.C **45**, 2094 (1992).
- [15] R.B. Wiringa, V.G.J. Stoks, R. Schiavilla, Phys. Rev. C **51**, 38 (1995).
- [16] D.R. Entem, R. Machleidt, Phys. Rev. C **66**, 014002 (2002); **68**, 041001(R) (2003).
- [17] E. Epelbaum, W. Glöckle, U.-G. Meissner, Nucl. Phys. **A747**, 362 (2005).
- [18] S.K. Bogner, T.T.S. Kuo, A. Schwenk, Phys. Rep. **386**, 1 (2003).
- [19] O. Plohl, C. Fuchs, E. N. E. van Dalen, Phys. Rev. C **73**, 014003 (2006)
- [20] J.A. Tjon, S.J. Wallace, Phys. Rev. C **32**, 267 (1985); Phys. Rev. C **32**, 1667 (1985).
- [21] R. Machleidt, Adv. Nucl. Phys. **19**, 189 (1989).
- [22] C.J. Horowitz, B.D. Serot, Nucl. Phys. **A464**, 613 (1987).
- [23] H. Müther, A. Polls, Prog. Part. Nucl. Phys. **45**, 243 (2000).